GUST ALLEVIATION ON A FORWARD SWEPT WING TRANSPORT AIRCRAFT

L. Klug[1], R. Heinrich[2]
T. Streit[2], R. Radespiel[1]
[1] Institute of Fluid Mechanics, TU Braunschweig, Braunschweig, 38108, Germany
[2] DLR Institute of Aerodynamics and Flow Technology, Braunschweig, 38108 Germany

Abstract

The paper describes and analyses potential concepts for gust alleviation at transonic speeds applied on a forward swept transport aircraft configuration. The main objective is to reduce structural weight by minimizing gust induced loads. Both inviscid and viscous aerodynamic simulations are performed for analysis. A gust study reveals a critical gust wave length of 50m leading to highest aerodynamic loads at cruise conditions. Gust induced separation is observed for particular cases. Deflection of a wing tip flap and the aileron at the outer wing have a remarkable short response time and offer strong flow actuation to reduce gust loads.

NOMENCLATURE

c	Reference chord length
C_L	Lift coefficient
C_D	Drag coefficient
C_{WBM}	Wing bending moment
c_p	Pressure coefficient
LE	Leading edge angle
M	Machnumber
SA	Spalart allmaras
t	time c
x,y,z	Cartesian coordinates
δ_{wt}	Deflection angle wing tip
$\delta_{wt,amp}$	Deflection angle amplitude wing tip
Φ_{LE}	Leading edge sweep angle
λ_{Gust}	Gust wave length
γ	dimensionless wing span
Γ	Lift Circulation
$V_{gust,amplitude}$	Gust amplitude

1. INTRODUCTION

There exists a strong interest in technologies for reducing the structural weight of commercial aircraft. Since the structural sizing is determined by gust loads and manoeuvring loads, concepts for alleviation of both loads must be developed. Due to the high flight speed, gust alleviation systems require fast actuators and must compensate gust-induced loads with short response time.

In general, gusts are relevant for many different aeronautical applications such as aircraft, helicopters, wind turbines and turbomachinery. Knowledge about unsteady aerodynamics and flow control can help to achieve supermaneuverability and enhanced aircraft agility [1,2]. As many aeronautical designs rely on laminar flow conditions, active gust allevation can reduce the risk of boundary layer transition caused by gusts, leading potentially to a more efficient aircraft [3]. Reduced loadings and vibrations on helicopter blades as well as an improved forward flight performance can be achieved by actively using moving control surfaces. It is the long term goal to couple moveable control surfaces with structural feedback strategies to actively control blade lift distribution [11]. Impacting pitching, yawing and rolling motion at the same time a complex three-dimensional as well as unsteady system has to be controlled [12]. From aerodynamic point of view active gust alleviation systems must offer high control authority and effectivity [13].

For exploiting the technology, the physical behaviour of dynamical actuated surfaces must be well understood. In the present paper a generic forward swept wing configuration was specifically designed for this purpose, based on the backward swept DLR LEISA research configuration. Previous studies with 1-cos gust representations have shown, that especially a forward swept wing can achieve fast change of lift along span [5].

The design process of the forward swept aircraft configuration is briefly explained in section 2, followed by description of the numerical setup and the used flow conditions. The gust simulation, presented in section 4 is subdivided in inviscid and a viscous analyses. The wing tip flap and aileron as potential gust alleviation actuators are described in section 5 followed by a short conclusion and outlook in section 6.

doi: 10.25967/530133

2. AIRCRAFT CONFIGURATION

Gust alleviation is investigated on the forward swept transport aircraft configuration shown in figure 1. This configuration is derived from the backward swept DLR LEISA configuration, explained in [5,6]. The wing tip flap coloured in red and the aileron coloured in green are used as gust alleviation actuators. The wing profile at the wing root is modified by redistributing thickness along the chord according to figure 2 in order to reduce shock induced separation.

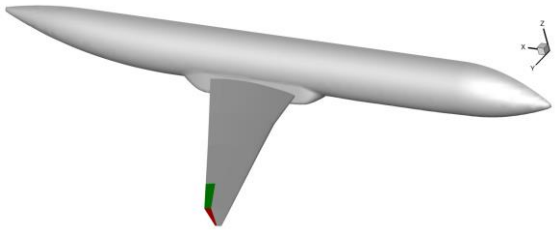

FIGURE 1. Forward swept configuration and gust Actuators

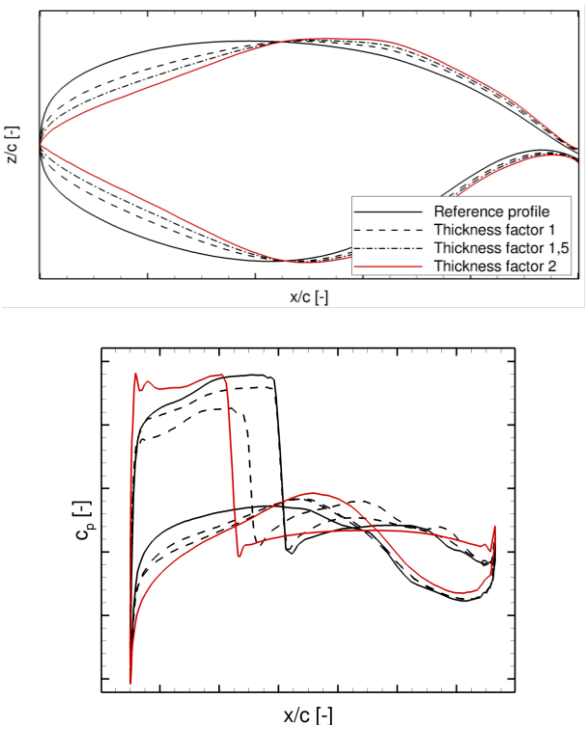

FIGURE 2. Effect of profile thickness on shock power

By redistributing thickness along the chord, a reduced suction peak can be noticed, according to figure 2. Nevertheless, this approach to minimize shock induced separation is somehow limited. Decreasing the thickness of the profile too much, results in a relatively sharp leading edge and an increased suction peak develops. This effect is coloured in red in figure 2.

Further shock reduction can be achieved by suited definition of the wing planform close to the wing root, shown in figure 3. Depending on the local leading edge angle, the separation region visualized by blue lines differs in terms of its location and extent. Based on the pressure distribution shown above a LE sweep of ~13° is finally chosen.

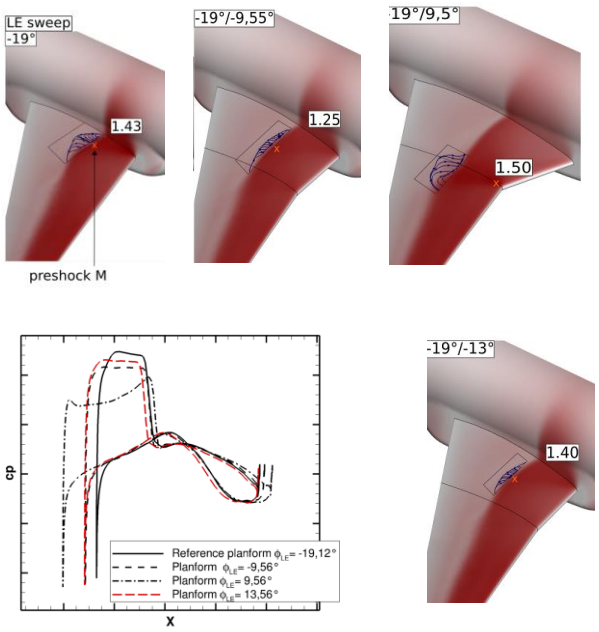

FIGURE 3. Effect of LE sweep angle of inner wing segment on shock strength and flow separation

3. NUMERICAL SETUP AND FLOW CONDITIONS

The numerical flow simulations make a discretization of the flow domain into finite cells necessary. This meshing is performed by CENTAUR 13.0. The expected boundary layers are resolved by introducing a layer of 50 prism cells. A non-dimensional distance of the cells near the wall of y^+ equal to 1 is approximately employed. Flow field solutions are computed by the DLR TAU 2018.1.0 code [10].

To reduce computational effort, half model simulations are performed. Cruise conditions, meaning Ma=0.8; H=35,000ft; C_L=0.5 are used in the present work. Figure 4 shows several slices through the viscous grid. A proper resolution of the transonic shock close to the fuselage wing interface is achieved by local cell clustering.

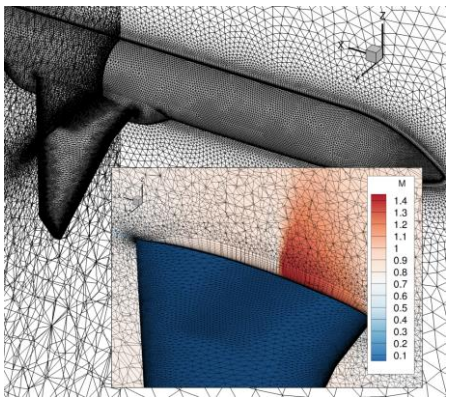

FIGURE 4. Viscous Grid

Dynamic flap deflection, as discussed in Chapters 5 and 6 is implemented by a TAU Python routine [7]. Blending areas between the non-deformed and deformed regions assure that the mesh deformation is done in a consistent way without introducing negative cells. The blending area was kept as small as possible, for arriving at a realistic surface representation compared to a real case application.

4. GUST SIMULATION APPROACH

Based on EASA CS 25 airworthiness requirements, atmospheric turbulences shown in figure 5 can be represented in a simplified manner [8,9]. Many load computations have shown that vertical disturbance velocities are the most critical cases for aerospace applications [6]. These vertical disturbance velocities have an common shape, meaning that 1-cos approximations can be applied. That is why in the current study, different wave lengths and amplitudes of a so called 1-cos gust are applied. Based on CS 25 a gust amplitude of 17,96m/s is used.

FIGURE 5a. 1-cos gust approximation by EASA CS 25

The numerical set up of a gust encounter takes into account the increased angle of attack by using a proven numerical approach for representing the gust [8]. In the following gust study, the gusts are superimposed with the flow field, beginning with a gust that starts ahead of the aircraft and then moves continuously over the aircraft, as shown in figure 5.

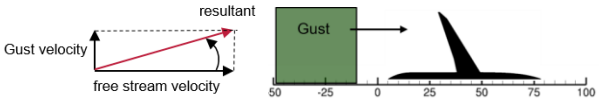

FIGURE 5b. Increased AoA due to gust encounter

4.1. Inviscid Gust Simulation

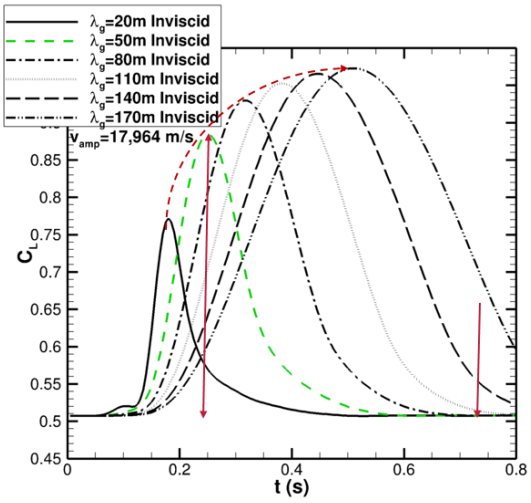

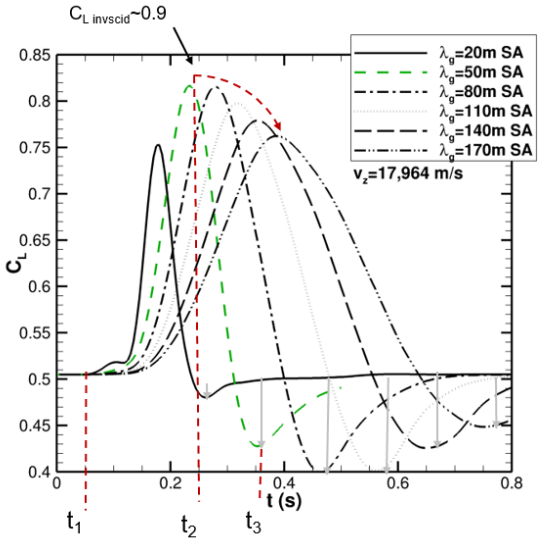

FIGURE 6. Inviscid vs. viscous RANS simulations

Inviscid gust simulations are performed in the beginning to describe the gas dynamical gust response, shown in figure 6. Lift increases during gust encounter. An asymptotic trend is noticed leading to a maximum increase of lift for long wave lengths.

4.2. Viscous Gust Simulation with RANS solutions

Viscous gust simulations show a very different trend. The maximum obtained lift decreases for wavelengths larger than 50m. Additionally, gust induced separation occurs, leading to transient lift reductions below the initial lift value. The flow field displayed at three different time instances reveals large separation regions during gust encounter, as shown in figure 7 and 8. In addition to gust induced separation, gust induced shock movement is noticeable; the shock moves far upstream during gust encounter.

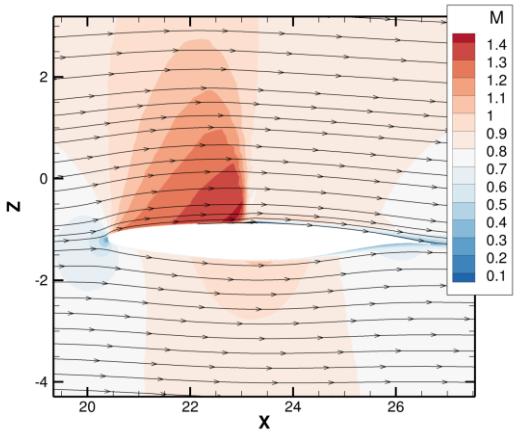

Gust induced transonic flow at t_1=0,1325s

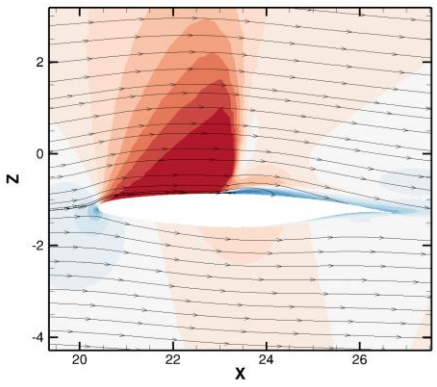

Gust induced separation at t_2=0,2325s

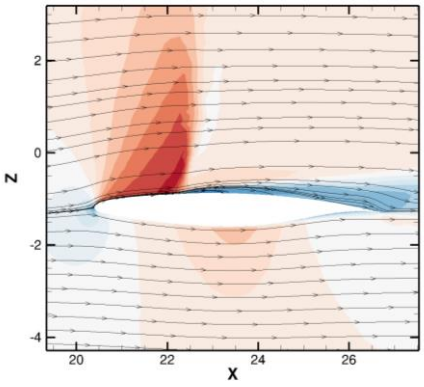

Gust induced separation at t_3=0,3525s

FIGURE 7: Gust induced separation at three times

Gust induced separation can be also observed by looking at the circulation distribution along span, as shown in figure 8. The separation occurs mainly in the inner part of the wing resulting in a strong loss of circulation. Figure 8 reveals that the initial increase of circulation during gust is highly nonlinear along the span. While the inner part of the wing experiences a relatively strong increase of lift, the increase at the outer part is relatively smaller.

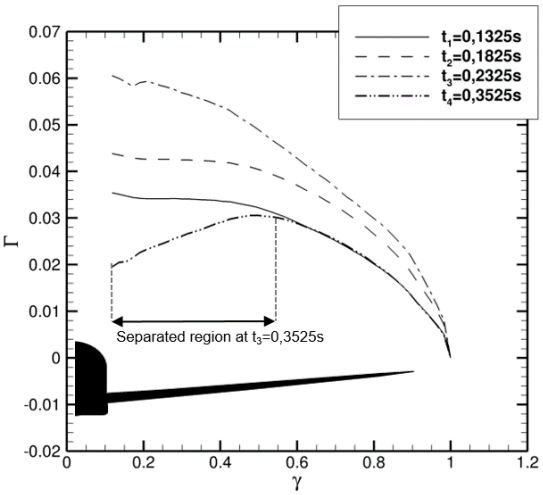

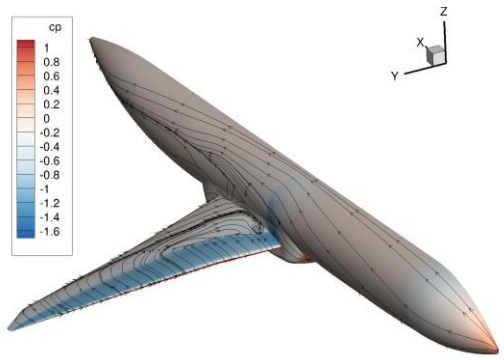

FIGURE 8: Surface streamlines at t=0,3525s and wing circulation during gust encounter

5. CONTROL FOR GUST ALLEVIATION

Two potential gust alleviation actuators are investigated, the wing tip flap and the aileron being placed right next to each other. The effect of both actuators is shown in following sections.

5.1. Wing Tip Flap

The wing tip flap, coloured in red in figure 9 is mounted at the outer part of the wing. Different deflection amplitudes and flap sizes are investigated. In the first step inviscid flow field calculations are used to analyse flow actuation. These simulations employed a sinusoidal flap deflection schedule.

FIGURE 9: Wing tip flap

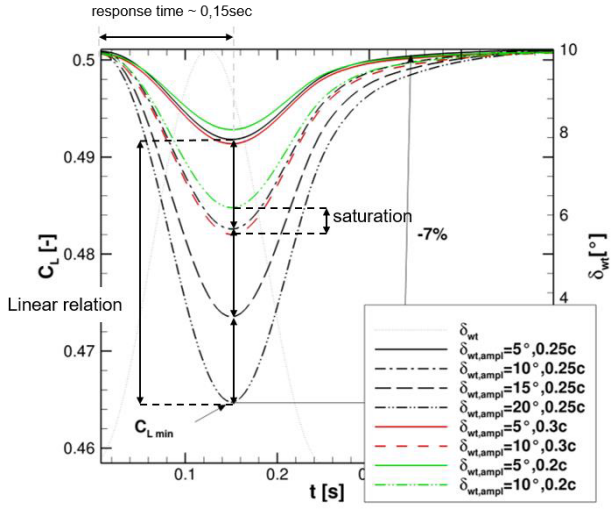

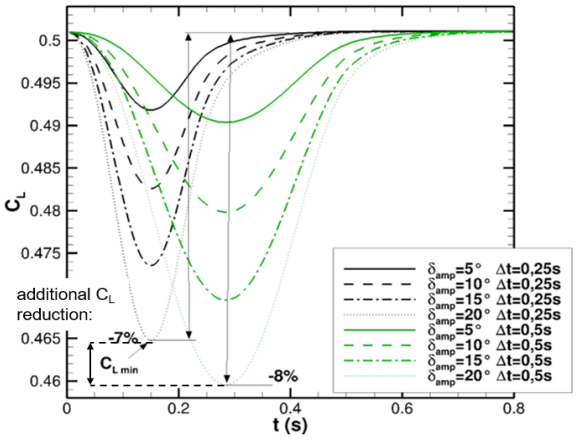

FIGURE 10: Wing Tip Flap - Parameter Study

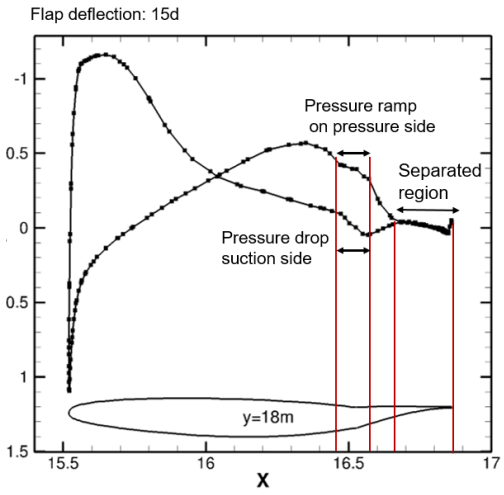

FIGURE 11. Lift dump and pressure distribution of wing tip flap - RANS

Figure 10 shows that increasing the flap size generally leads to larger control authority. However, the achieved lift decreases display an asymptotic trend with increasing flap chord. Also, the slower actuation cycle resulted in significantly higher lift dumps. We conclude that flap chord lengths of 25% and sinusoidal transients with a wave length of 0.25s seem to be physics based limits of flap actuation.

Taking viscous effects into account, flow separation at the wing tip flap is monitored, as shown in figure 11. Consequently, a reduced lift dump compared to assuming inviscid flow occurs. The pressure distribution along the wing chord at 90% of wing span indicates, that about 70% chord of the flap is separated.

An extremely important result of flow actuation is the achieved reduction of wing bending moment. In present case, two coordinate systems are defined. The so called y45c system reflects the wing bending moment along span. The reference bending line connects the 45% chord positions of the wing tip and the wing root, as illustrated in figure 12. The yr-value represents the wing-fuselage interface, meaning that the bending moment is computed around the x-axis positioned at the wing root. In total a reduction of roughly 10% at the wing root can be achieved by a deflection of the wing tip flap by 15°.

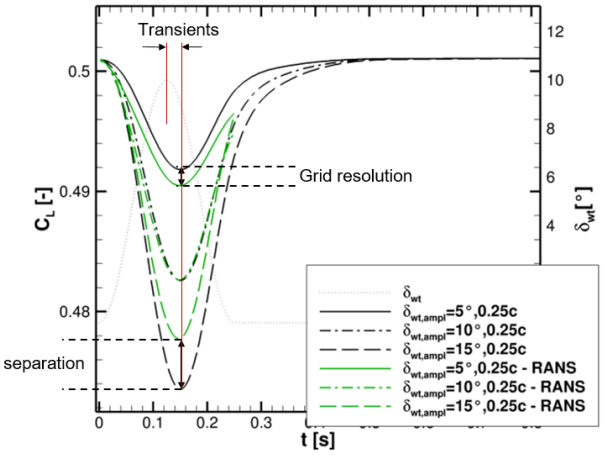

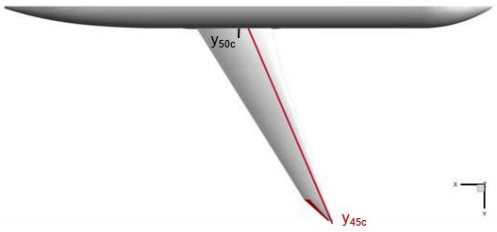

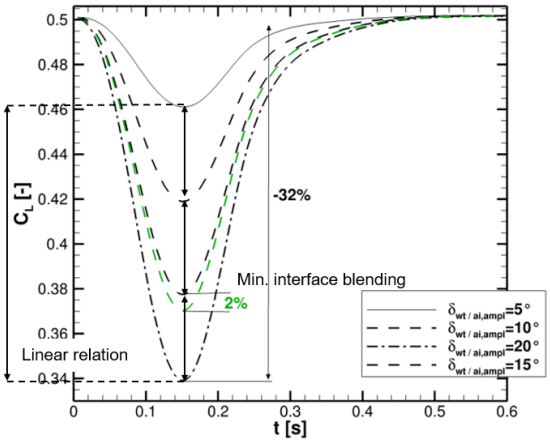

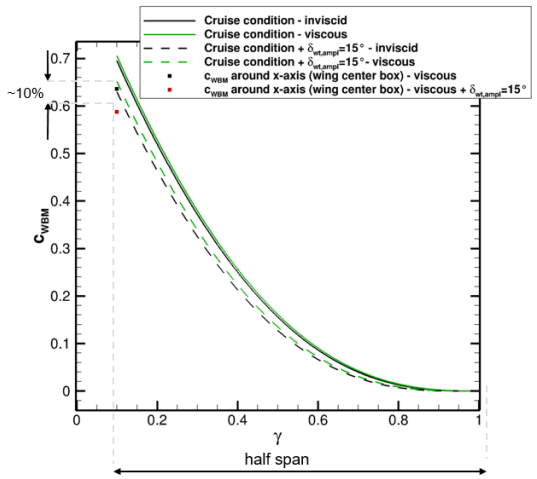

FIGURE 12. Trend of wind bending moment for wing tip flap and aileron

5.1. Wing Tip Flap and Aileron

In the next step, the aileron is additionally taken into account, as displayed in figure 1. The aileron has a local depth of 25% wing chord. Once again the lift dump and the reduced wing bending moment are considered. Compared to the deflection of the wing tip flap alone, Figure 13 shows that the aileron increases the lift dump by a factor of roughly four. In total, the combined effect of wing-tip flap and aileron reduces the wing bending moment at the wing-fuselage interface by 35%.

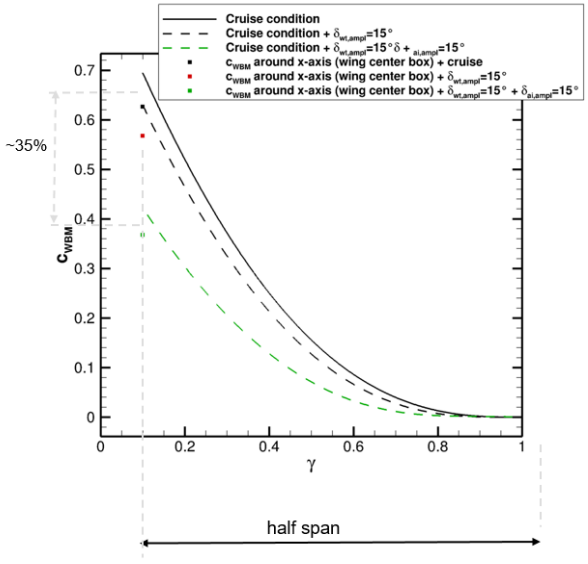

FIGURE 13. Actuation of wing tip flap and aileron

6. CONCLUSION AND OUTLOOK

During encounter of large gusts according to CS25 significant flow separations on the wing are observed at cruise conditions. The flow needs a relatively long time to recover, and a complex, nonlinear transient of lift over the span develops. This phenomenon cannot be simulated by inviscid methods, so that viscous RANS simulations are mandatory for gust simulation at transonic speeds.

Our current simulations show that control surfaces close to the wing tip, e.g. wing tip flaps and ailerons are effective to reduce control the wing root bending moment.

By deflecting a wing tip flap the wing bending moments are reduced by roughly 10%. Large deflection angles, however, lead to flow separation at the lower surface of the wing tip flap. Actuation schedules with a temporal length of 0.25s or longer appear to be effective. Much higher control effectiveness is gained by including the aileron into the flow actuation approach. In that case, wing bending moments can be reduced by 35%.

Future work will focus on the deflection of droop noses to compensate gust-induced wing torsion moments. That will include assessment of different deflection amplitudes as well as deflection speeds. Finally, both leading and trailing edge devices will be employed simultaneously to achieve effective gust alleviation.

REFERENCES

[1] W.J. McCroskey, P.M. Goorjian, Interaction of Airfoils with Gusts and Concentrated vortices in unsteady Transonic Flow, AIAA-83-1691,1983

[2] R.M. Rennie, E.J. Jumpert, Experimental Measurements of Dynamic Control Surface Effectivenes, Journal of Aircraft, Vol. 33, No. 55, 1996

[3] Caleb J. Bames, M. R. Visbald, Further Investigations of Vortical-Gust/Airfoil Interactions at a Transitional Reynolds Number, AIAA 2018-0823

[4] X. He, C. Fuentes, W. Shyy, Y. Lian and b. Caroll, Computation of Transitional Flows around Airfoil with a moveable flap, AIAA 2000-2240

[5] L. Klug, R. Radespiel, J. Ullah, F. Seel, T. Lutz, J. Wild, R. Heinrich, T. Streit, Actuator concepts for active gust alleviation on transport aircraft at transonic speeds, AIAA 2020-0271

[6] J. Wild, An integrated design approach for lonoisexposing high-lift devices, 3rd AIAA Flow Control Conference, AIAA, 2006

[7] R. Heinrich, L. Capsada, Development of the DLR TAU code for modelling of control surfaces, DLRK, 2018

[8] R.]Heinrich, “Simulation of interaction of aircraftand gust using the TAU-code,” New Results in Numerical and Experimental Fluid Mechanics IX, Springer, 2014, pp. 503–511.

[9] EASA, “Certification Specifications for Large Aeroplanes (CS-25). Amendment 3,” European Aviation Safety Agency, 2007.

[10] TAU-Code User Guide. Release 2018.1.0, July 2018

[11] Leishmann, J. G., “Unsteady Lift of a Flapped Airfoil by Indicial Concepts,” Journal of Aircraft–Vol. 31, No. 2, 1994.

[12] Lian, Y., “Numerical Study of a Flapping Airfoil in Gusty Environments,” AIAA Paper 2009–3952, 2009

[13] Qiang Zhou, Y. L., Gang Chen, and Ronch,A.D., “Aeroelastic Moving Gust Responses and Alleviation based on CFD,” AIAA Paper 2016–3837, 2016.